# Distributed measurements of fiber birefringence and diametric load using optical low-coherence reflectometry and fiber gratings

**Dragan Coric, Hans G. Limberger, and René P. Salathé**

*Ecole Polytechnique Fédérale de Lausanne (EPFL), Advanced Photonics Laboratory, CH-1015 Lausanne, Switzerland*
hans.limberger@epfl.ch

**Abstract:** Polarization sensitive optical low-coherence reflectometry (OLCR) is used for measuring the complex fiber Bragg gratings (FBG) reflection coefficient. We determine the beat length directly from oscillations in the OLCR amplitude with a resolution of $10^{-6}$ and a spatial resolution only limited by the minimum beat length or the coherence length of the light source. Using the OLCR amplitude and phase in combination with an inverse scattering algorithm the birefringence is retrieved with a resolution of $2\times10^{-5}$ while the spatial resolution is 25 μm. The two developed techniques are applied for measuring position, magnitude and footprint of induced birefringence of an FBG under uniform and non-uniform diametric loading.



**OCIS codes:** (230.1480) Bragg reflectors; (120.3180) Interferometry; (260.1440) Birefringence; (060.2270) Fiber characterization.

## References and links

1. P. Lambelet, P. Y. Fonjallaz, H. G. Limberger, R. P. Salathé, C. Zimmer, and H. H. Gilgen, "Bragg grating characterization by Optical Low-Coherence Reflectometry," IEEE Photon. Technol. Lett. **5**, 565-567 (1993).
2. P. Giaccari, H. G. Limberger, and R. Salathé, "Local characterization of fiber Bragg gratings complex coupling coefficient," Opt. Lett. **28**, 598-600 (2003).
3. S. D. Dyer and K. B. Rochford, "Low-coherence interferometric measurements of fibre Bragg grating dispersion," Electron. Lett. **35**, 1485-1486 (1999).
4. P. Giaccari, "Fiber Bragg gratings characterization by Optical Low-Coherence Reflectometry and sensing applications," *Microengineering Department, Swiss Federal Institute of Technology Lausanne*, PhD thesis no. 2726, Lausanne (2003).
5. R. Feced, M. N. Zervas, and M. A. Muriel, "An efficient inverse scattering algorithm for the design of nonuniform fiber Bragg gratings," IEEE J. Quantum Electron. **35**, 1105-1115 (1999).
6. J. Skaar, L. Wang, and T. Erdogan, "On the synthesis of fiber Bragg gratings by layer peeling," IEEE J. Quantum Electron. **37**, 165-173 (2001).
7. M. Volanthen, H. Geiger, M. J. Cole, and J. P. Dakin, "Measurement of arbitrary strain profiles within fiber gratings," Electron. Lett. **32**, 1028-1029 (1996).
8. M. M. Ohn, S. Y. Huang, R. M. Measures, and J. Chwang, "Arbitrary strain profile measurement within fibre gratings using interferometric Fourier transform technique," Electron. Lett. **33**, 1242-1243 (1997).
9. P. Giaccari, G. R. Dunkel, L. Humbert, J. Botsis, H. G. Limberger, and R. P. Salathé, "On direct determination of non-uniform internal strain fields using fibre Bragg gratings," Smart Mater. Struct. **14**, 127-136 (2005).
10. F. Bosia, P. Giaccari, J. Botsis, M. Facchini, H. G. Limberger, and R. Salathé, "Characterization of the response of fibre Bragg grating sensors subjected to a two-dimensional strain field," Smart Mater. Struct. **12**, 925-934 (2003).
11. R. B. Wagreich, W. A. Atia, H. Singh, and J. S. Sirkis, "Effects of diametric load on fibre Bragg gratings fabricated in low birefringent fibre," Electron. Lett. **32**, 1223-1224 (1996).
12. X. Shu, K. Chisholm, I. Felmeri, K. Sugden, A. Gillooly, Z. Lin, and I. Bennion, "Highly sensitive transverse load sensing with reversible sampled fiber Bragg gratings," Appl. Phys. Lett. **83**, 3003-3005 (2003).

#74850 - $15.00 USD Received 7 September 2006; revised 7 November 2006; accepted 8 November 2006

13. P. Torres and L. C. G. Valente, "Spectral response of locally pressed fiber Bragg grating," Opt. Commun. **208**, 285-291 (2002).
14. S. C. Tjin, L. Mohanty, and N. Q. Ngo, "Pressure sensing with embedded chirped fiber grating," Opt. Commun. **216**, 115-118 (2003).
15. M. Leblanc, S. T. Vohra, T. E. Tsai, and E. J. Friebele, "Transverse load sensing by use of pi-phase-shifted fiber Bragg gratings," Opt. Lett. **24**, 1091-1093 (1999).
16. A. M. Gillooly, H. Dobb, Z. Lin, and I. Bennion, "Distributed load sensor by use of a chirped moire fiber Bragg grating," Appl. Opt. **43**, 6454-6457 (2004).
17. D. Sandel, R. Noe, G. Heise, and B. Borchert, "Optical network analysis and longitudinal structure characterization of fiber Bragg grating," J. Lightwave Technol. **16**, 2435-2442 (1998).
18. O. H. Waagaard, "Polarization-resolved spatial characterization of birefringent Fiber Bragg Gratings," Opt. Express **14**, 4221-4236 (2006).
19. O. H. Waagaard and J. Skaar, "Synthesis of birefringent reflective gratings," J. Opt. Soc. Am. A **21**, 1207-1220 (2004).
20. K. Takada, J. Noda, and R. Ulrich, "Precision measurement of modal birefringence of highly birefringent fibers by periodic lateral force," Appl. Opt. **24**, 4387-4391 (1985).
21. A. Simon and R. Ulrich, "Evolution of polarization along a single-mode fibre," Appl. Phys. Lett. **31**, 517-520 (1977).
22. K. Takada, A. Himeno, and K.-i. Yukimalsu, "High sensitivity and submillimeter resolution optical time-domain reflectometry based on low-coherence interference," J. Lightwave Technol. **10**, 1998-2005 (1992).
23. D. P. Dave and T. E. Milner, "Precise beat length measurement of birefringent fibres with dual channel low-coherence reflectometer," Electron. Lett. **37**, 215-216 (2001).
24. B. Huttner, J. Reecht, N. Gisin, R. Passy, and J. P. Von der Weid, "Local birefringence measurements in single-mode fibers with coherent optical frequency-domain reflectometry," IEEE Photon. Technol. Lett. **10**, 1458-1460 (1998).
25. A. Galtarossa, L. Palmieri, A. Pizzinat, M. Schiano, and T. Tambosso, "Measurement of local beat length and differential group delay in installed single-mode fibers," J. Lightwave Technol. **18**, 1389-1394 (2000).
26. B. J. Soller, D. K. Gifford, M. S. Wolfe, and M. E. Froggatt, "High resolution optical frequency domain reflectometry for characterization of components and assemblies," Opt. Express **13**, 666-674 (2005).
27. D. Coric, H. G. Limberger, and R. P. Salathé, "Direct measurement of fiber Bragg grating local birefringence using optical low coherence reflectometry," in *17th International Conference on Optical Fibre Sensors, OFS'17*, Proc. of SPIE **5855**, 154-157, Bruges (2005).
28. D. Coric, H. G. Limberger, and R. P. Salathé, "Distributed sensing of diametric load using Optical Low Coherence Reflectometry and fiber Bragg gratings," in *Bragg Gratings, Photosensitivity, and Poling in Glass Waveguides, BGPP/ACOFT'2005*, Sydney (2005).
29. R. J. Espejo and S. D. Dyer, "High spatial resolution measurements of transverse stress in a fiber Bragg grating using four-state analysis low-coherence interferometry and layer-peeling," Proc. SPIE **6167**, 616707, San Diego, CA, United States (2006).
30. Y. Namihira, "Opto-elastic constant in single mode optical fibers," J. Lightwave Technol. **LT-3**, 1078 (1985).

## 1. Introduction

Optical low coherence reflectometry (OLCR) is an interferometric technique that allows measuring amplitude and phase of the light reflected from the device under test. OLCR was proved to be a powerful tool for the determination of the various properties of fiber Bragg gratings (FBG), such as position, length [1], and impulse response [2] from which the wavelength spectrum or group delay are obtained by Fourier transformation [3, 4]. Using the measured impulse response, it is possible to retrieve the complex coupling coefficient of the grating, $q(z)$, through inverse scattering algorithms, such as layer-peeling [5, 6]. The complex coupling coefficient contains information about the refractive index modulation and the local grating period along the grating length. The possibility to monitor changes in local FBG parameters opened new possibilities for high spatial resolution grating characterization and distributed sensing [4, 7-10]. The complete characterization and sensing applications of the FBG using high-resolution reflectometry methods were mostly limited so far to non-birefingent gratings.

However, for many applications it is desirable to have birefringent FBGs, such as gratings written in polarization maintaining (PM) fibers. Birefringence can also be induced when the

#74850 - $15.00 USD Received 7 September 2006; revised 7 November 2006; accepted 8 November 2006

grating is exposed to external influences, such as diametric loading [10, 11]. Different grating types have already been used including sampled [[12] chirped [13, 14], and phase shifted gratings [15] to measure distributed, applied load. Common to all these techniques is the fact that they analyze changes in reflection spectra to get information about the induced birefringence, which is directly related to the applied load [11]. Gillooly *et al.* [16] demonstrated a load sensor based on a chirped Moiré grating which is able to measure position, magnitude and footprint of the load with a spatial resolution of 160 μm.

When the polarization state and principal polarization axis along the grating changes arbitrarily (non-uniform birefringence, twist etc), it is necessary to measure the complete reflection Jones matrix and to apply vector layer-peeling algorithm to completely characterize the FBG [17-19]. On the other side, if the polarization states along the grating axes stay constant scalar methods can be used, and the grating can be decomposed into two gratings along the two independent axes. Such birefringent FBGs support two distinct polarization eigenmodes with two effective refractive indices, $n_S$ and $n_F$. Light propagating on the orthogonal axis experiences two different Bragg wavelengths corresponding to slow (S) and fast (F) axes: $\lambda_S = 2\, n_S\, \Lambda$ and, $\lambda_F = 2\, n_F\, \Lambda$; where, $\Lambda$, is the period of the grating. The FBG birefringence, $B = n_S - n_F$, is usually obtained from the spectral measurement as a difference in the wavelength peaks and the grating period:

$$B = \frac{\lambda_S - \lambda_F}{2\Lambda} \tag{1}$$

Such a measurement gives the phase birefringence averaged over the length of the grating, limiting the spatial resolution. An equivalent parameter for describing the phase modal birefringence along the fiber is the beat length $L_B$ defined as:

$$L_B = \frac{\lambda}{B} \tag{2}$$

where $\lambda$ is the operating wavelength. The beat length signifies the length over which the state of the polarization of the light makes one full circle inside the fiber. The beat length is usually measured using localized perturbations such as mechanical pressure [20] or magnetic field [21]. The birefringence B in an FBG contains three parts, the intrinsic fiber birefringence, the birefringence induced by the UV writing process, and the birefringence induced by external force.

High sensitivity OLCR was already used to determine fiber beat length by measuring oscillations in the Rayleigh backscattering signal [22], or reflection from the fiber end [23]. Other reflectometery methods such as optical frequency domain reflectometry (OFDR) [24] and optical time domain reflectometry (OTDR) [25] were also used for measuring beat length with resolution on centimeter and meter scale, respectively. While OLCR measures the impulse response (time domain), the OFDR measures the frequency response (spectral domain). Both are linked by Fourier transformation. Recently Soller *et al.* [26] used a polarization and phase sensitive OFDR to extract the beat length of a low birefringent FBG (16 cm beat length) from amplitude oscillations in the grating impulse response, which was obtained from the measured complex (phase and amplitude) reflectivity by a Fourier transformation.

In this article we present high-resolution measurements of the distributed beat length (method 1) and phase birefringence (method 2) of an FBG using the OLCR technique. First, the beat length was measured directly from the OLCR amplitude, without the need of the phase sensitive part of the setup. Next, using both, the OLCR amplitude and phase together with an inverse scattering algorithm the local birefringence was retrieved with high spatial resolution. To illustrate the possibilities of the method we measured first FBG beat length and phase birefringence of a PM fiber. Second, the FBG birefringence and beat length induced by uniform and non-uniform diametric loading in a low birefringent standard single mode fiber

#74850 - $15.00 USD Received 7 September 2006; revised 7 November 2006; accepted 8 November 2006

was investigated. We reported a part of this work on two conferences [27, 28]. In the mean time Espejo an Dyer have reported similar OLCR phase birefringence measurements on a conference this year [29].

## 2. Experimental setup and methodology

The scheme of the OLCR setup is shown in Fig. 1 Light from the superluminescent diode (Exalos, Gaussian spectral profile, center wavelength 1550 nm, 50 nm spectral width) and tunable laser (Tunics, Photonetics) are time multiplexed, and split in the reference and test arm using a 50/50 directional coupler. The tunable laser provides a reference for the phase measurement and in the same time allows for measurements of the grating transmission and reflection spectra.

Light from the reference and test arm is reflected back and interferes inside the coupler (CPL) only if the length difference of the two arms is smaller than the coherence length of the light source. Scanning the mirror in the reference arm, the FBG in the test arm is probed with a resolution determined by the spectral width of low-coherence source. The light is detected using two photodiodes in a balanced detection scheme (BD) and a lock-in amplifier (LIA), which is set to the frequency of the piezoelectric phase modulator (PEM) [2] . Compared to the set-up we used in Ref. [2], the polarizer (POL) is now introduced in the test arm to probe gratings on the specific fiber axis. For each polarization, the light intensity is maximized by adjusting polarization controller PC2. Finally, the visibility of the interferometric signal is optimized using polarization controller PC1 in the reference arm. The setup allows measurements with high sensitivity (-120 dB) and spatial resolution (25 μm). More details on the general performance of our system can be found in Refs. [2] and [9].

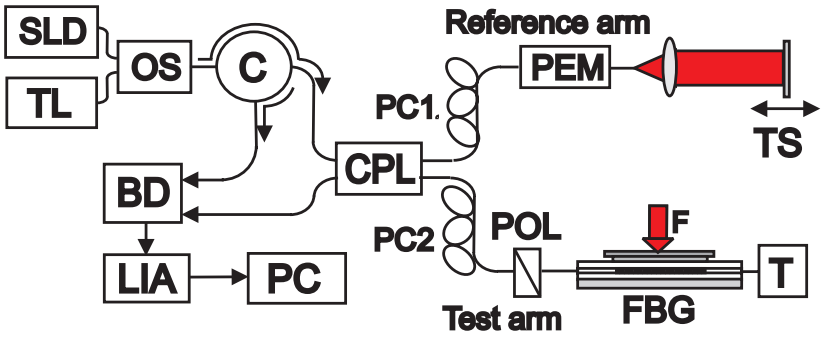


Fig. 1. Scheme of the optical low-coherence reflectometer. SLD: superluminescent diode; TL: tunable laser; OS: optical switch; C: circulator; PEM: piezoelectric modulator; TS: translational stage; FBG: grating under test; CPL: 3 dB coupler; BD: balanced detector; POL: polarizer; PCL1 and PCL2: polarization controllers; T: transmission spectra detector.

The described amplitude and phase-sensitive OLCR allows for measuring the impulse response of the device under test directly [2]. The wavelength spectrum and group delay are obtained by Fourier transformation [4]. Time domain layer-peeling is then applied to calculate the complex coupling coefficient, *q(z)* [6]. Using this complex coupling coefficient it is possible to calculate the local grating parameters such as index modulation amplitude, $\Delta n_{ac}$, effective Bragg wavelength, $\lambda_{eff}$, and background index, $\Delta n_{dc,}$ using the following equations [4]:

$$\Delta n_{ac}(z) = \frac{\lambda_D}{\eta\pi}\left|q(z)\right| \tag{3}$$

#74850 - $15.00 USD Received 7 September 2006; revised 7 November 2006; accepted 8 November 2006

$$\lambda_{eff}(z) = \left( \frac{1}{\lambda_D} + \frac{1}{4\pi \cdot n_{eff}} \frac{d\phi_q(z)}{dz} \right)^{-1} \tag{4}$$

$$\Delta n_{dc}(z) = \frac{\lambda_D}{4\pi \cdot \eta} \left( \frac{d\theta(z)}{dz} - \frac{d\phi_q(z)}{dz} \right) \tag{5}$$

where $\eta$ is a fraction of the modal power that is contained in the fiber core; $\lambda_D$ is the design Bragg wavelength; $\phi_q(z) = \arg\left(q(z)\right)$ is the coupling coefficient phase and $\theta(z)$ the grating period chirp. Assuming that the period chirp is constant we get:

$$\Delta n_{dc}(z) = -\frac{\lambda_D}{4\pi \cdot \eta} \frac{d\phi_q(z)}{dz} \tag{6}$$

Changes of the grating period chirp do not contribute to the measured birefringence since they are equal along both main axes. Measuring the local grating parameters on various polarization axes (two main axes and in-between) it is possible to get high spatial resolution information on the grating natural or induced birefringence. The phase sensitive measurement provides complete grating characterization, but the amplitude measurement is simpler and could also provide, as it will be shown, useful information regarding the FBG birefringence. In all measurements we assume that the UV induced grating birefringence is much smaller than the fiber natural (due to the fabrication process) or induced birefringence (diametric loading). In this way we can still use scalar methods, since there are two well defined main axes. The role of the grating is to enhance the reflectivity from the fiber. The OLCR reflectivity signal inside a typical FBG is -50 dB compared to -120 dB for fiber Rayleigh scattering.

## 3. Results and discussion

The described OLCR setup was used to measure three samples. First, a uniform Bragg grating written in a polarization maintaining (PM) fiber was measured. This grating served as a sample to demonstrate the two methods (3.1). Next, a uniform grating in non-birefringent fiber was exposed to a uniform load over the whole grating length (3.2). The goal of this measurement was to compare OLCR with traditional spectral methods for measuring the transversal load induced birefringence. To further demonstrate the possibilities of the presented technique, a uniform grating in a non-birefringent fiber was exposed to non-uniform load (3.3). In this case the spectral methods cannot provide direct information about the load configuration.

### *3.1 Characterization of the fiber Bragg grating written in polarization maintaining fiber*

a) Beat length measurement

The test FBG was a commercial (Avensys) grating written in high-birefringent PM fiber (Panda Fujikura). The grating length was 7.5 mm and the peak reflectivity was 63%, with an average index modulation of $2\times10^{-4}$. Using the described OLCR set-up, the PM-FBG was probed using linearly polarized light on the two main axes as well as on the various angles in-between. It should be noted that in this set of measurements it is not necessary to use phase sensitivity of the OLCR. This considerable simplifies the setup complexity and decreases measurement and processing (Such measurement could be performed using commercially available reflectometers). Figure 2 shows the OLCR amplitude for probing along the fast and the 45 degrees fiber axis, respectively. When the FBG is probed on an axis different from one of the principal axes, oscillations in the OLCR amplitude signal appear. The highest visibility

#74850 - $15.00 USD Received 7 September 2006; revised 7 November 2006; accepted 8 November 2006

is achieved when the polarization state is 45 degree relative to the principal axes. Oscillations in the OLCR signal come from the fact that light coupled off the main axes of the PM fiber rotates its state of polarization. This oscillation period, $\Delta z$, is equal to half of the local beat length, because the detected light travels back and forth in the grating [22]. From the oscillations inside the PM grating we measured a beat length of $L_B = 2\,\Delta z = 4.22\pm0.05$ mm, which corresponds to a birefringence of $(3.67\pm0.04)\times10^{-4}$. This value is well within the specification range of the PM-fiber birefringence. Corresponding transmission spectra showed a clear splitting as a typical signature of birefringence. From this splitting, a birefringence of $(3.6\pm0.2)\times10^{-4}$ can be evaluated from the wavelength difference $\Delta\lambda$. The spectral measurement error is due to the uncertainty in peak wavelength determination (±20 pm). The difference between the two birefringence values is 0.5%, which indicates that local beat length and birefringence can be correctly obtained from the OLCR amplitude.

The minimum measurable birefringence is limited by the maximum beat length which should be smaller than two times the grating length, i.e. $B_{min} = \lambda_D / (2\,L_{FBG})$. For a 10-mm-long grating the minimal birefringence is $7.8\times10^{-5}$ at 1.55 μm. In principle it would be possible to reduce this value further by using the light that undergoes multiple reflections and appears behind the grating.

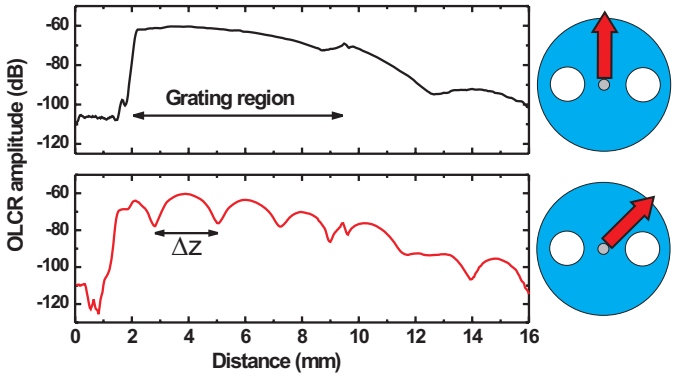


Fig. 2. OLCR Amplitude as a function of geometrical distance along uniform Bragg grating written in PM fiber; Probing on the fast axis (top), probing at 45 degrees (bottom).

b) Birefringence measurement

The distributed phase birefringence can be obtained from the OLCR amplitude and phase measurement together with the calculated local Bragg wavelength for small index changes, i.e. $\left|\Delta n_{eff} / n_{eff}\right| \ll 1$ using Eq. (4) and (6):

$$B(z) = \frac{\lambda_{eff,S}(z) - \lambda_{eff,F}(z)}{2\,\Lambda} \tag{7}$$

The local Bragg wavelength for the main axes and the resulting birefringence are plotted as a function of the geometrical distance in Fig. 3. To avoid a position offset between two main axes along the grating, which could lead to artifacts in the obtained birefringence, both measurements were aligned with respect to the entrance of the FBG using the OLCR amplitude signals (micrometer precision).

#74850 - $15.00 USD Received 7 September 2006; revised 7 November 2006; accepted 8 November 2006

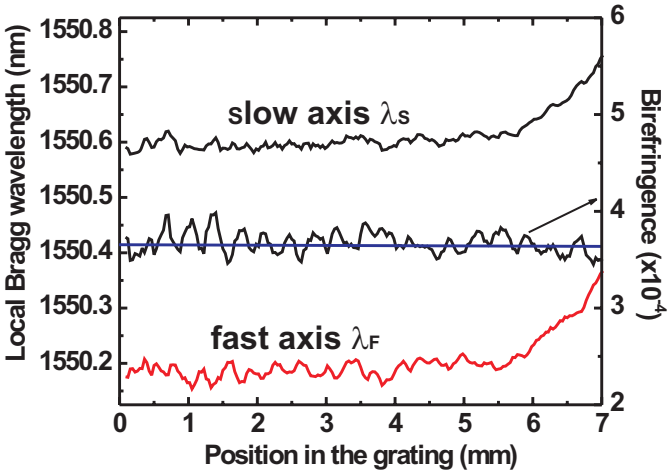


Fig. 3. Local Bragg wavelength for two main axis of PM-FBG (left) and birefringence (right), as a function of a position in the grating (obtained from OLCR measurement and inverse scattering).

This method requires two independent OLCR (amplitude and phase) measurements along the principal axes. However, it provides high spatial resolution limited by the coherence length of broadband light source, which in our case is 25 μm (The curves in Fig. 3 are filtered using a Hamming window which reduces the spatial resolution to 100 μm). The mean local birefringence within the grating is $3.6\times10^{-4}$ with a $3\sigma$ deviation of $3\times10^{-5}$. We can observe a good agreement with the mean birefringence value obtained from the reflection spectra (blue line in Fig. 3). Using the OLCR measurement in combination with inverse scattering algorithm the local Bragg wavelength can be measured with a maximum error of ±10 pm [9]. Therefore the minimum birefringence is retrieved with an error of about $2\times10^{-5}$.

### *3.2 Uniform diametric load of fiber Bragg grating written in standard fiber*

To test the direct method of beat length measurement from the OLCR amplitude a non-birefringent FBG was exposed to transverse load. The 7-mm-long grating was fabricated in a germanosilicate fiber with 18mol% $GeO_2$ using ArF excimer laser radiation and phase mask technique. Grating reflectivity and index modulation amplitude were 65% and $2\times10^{-4}$, respectively. The measured beat length (birefringence) provides information for the calculation of transverse strain [10, 11].

For every load the OLCR amplitude and reflection spectrum were measured (since the loading setup is not calibrated, the loading values are given in arbitrary units). Loading of the grating induces oscillations in the OLCR amplitude. Its period is directly related to the beat length. Therefore, by measuring the oscillation period it is possible to calculate the induced birefringence (Fig. 4 black squares) using Eq. (2) between birefringence and beat length (black curve). The comparison with the spectral measurement (red dots) gives very good agreement within the measurement error of the tunable laser (20 pm).

#74850 - $15.00 USD Received 7 September 2006; revised 7 November 2006; accepted 8 November 2006

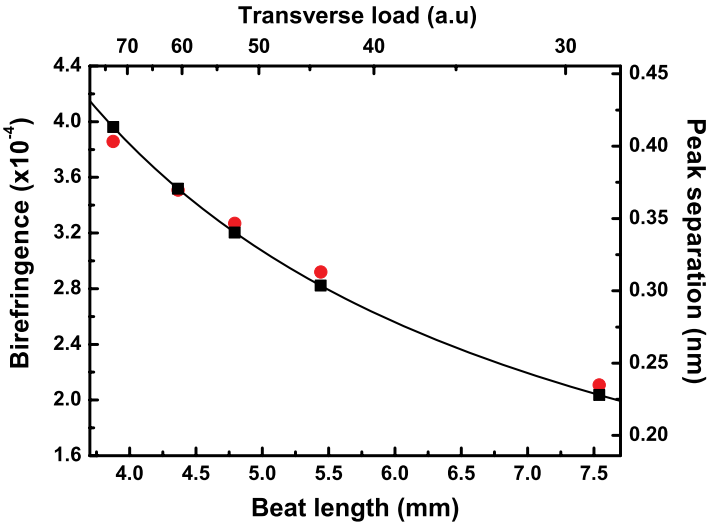


Fig. 4. Induced birefringence as a function of beat length and load during uniform FBG loading (spectral measurements, red circles, are shown for a comparison).

### *3.3 Non-uniform diametric load of fiber Bragg grating written in standard fiber*

Here we compare both, the measurement of local beat length (method 1) and phase birefringence (method 2) for distributed diametric load. A 30-mm-long FBG in a single mode fiber (SMF-28) with 75% reflectivity, an index modulation amplitude of $0.7\times10^{-4}$ was used. The loading element had 2 loading sections of 2 mm length each separated by 2 mm. Figure 5(a) shows the OLCR amplitude measurement for probing along the 45 degrees fiber axis with and without loading. The two loading sections can clearly be identified by pronounced amplitude oscillations. From these oscillations in the amplitude signal it is possible to determine the birefringence (as explained in section 3.1), averaged over half a beat length period. The spatial resolution of the beat length (or birefringence) increases with applied load (more oscillations per unit length), and ranges from the OLCR resolution up to the grating length. Figure 5(b) shows the OLCR phase along the fiber Bragg grating under load. Both, in the amplitude (Fig. 5(a)) and in the OLCR phase signal (Fig. 5b) the boundaries of the loading sections can be resolved directly (black vertical lines) with 25 μm resolution.

The transversal stress induces a change of the background index $\Delta n_{dc}$ and the local Bragg wavelength. From the measured impulse response, using Eq. (6), it is possible to calculate the birefringence along the grating with spatial resolution given by the coherence length of the light source and the filter function. Figure 5c shows a comparison of birefringence obtained from the OLCR amplitude and the phase. The agreement between the two methods is very good. Differences are within the respective errors. As the load element was manufactured with loading sections of slightly different heights, the load was not uniformly distributed between the two sections. The applied force (right axis in Fig. 5(c)) can be calculated from photo-elastic theory leading to a direct relation between induced birefringence $B$ and applied load per unit length $F_L$ [30]:

$$B = \frac{8C}{\pi d} F_L \tag{7}$$

#74850 - $15.00 USD Received 7 September 2006; revised 7 November 2006; accepted 8 November 2006

where $d$ =125 μm is fiber diameter, and $C$= $3.08\times10^{-12}$ $m^2$ $N^{-1}$ the photo-elastic constant at 1.55 μm [30]. Maximum load values for the first and second loading elements are 34.4 and 12.4 N/mm.

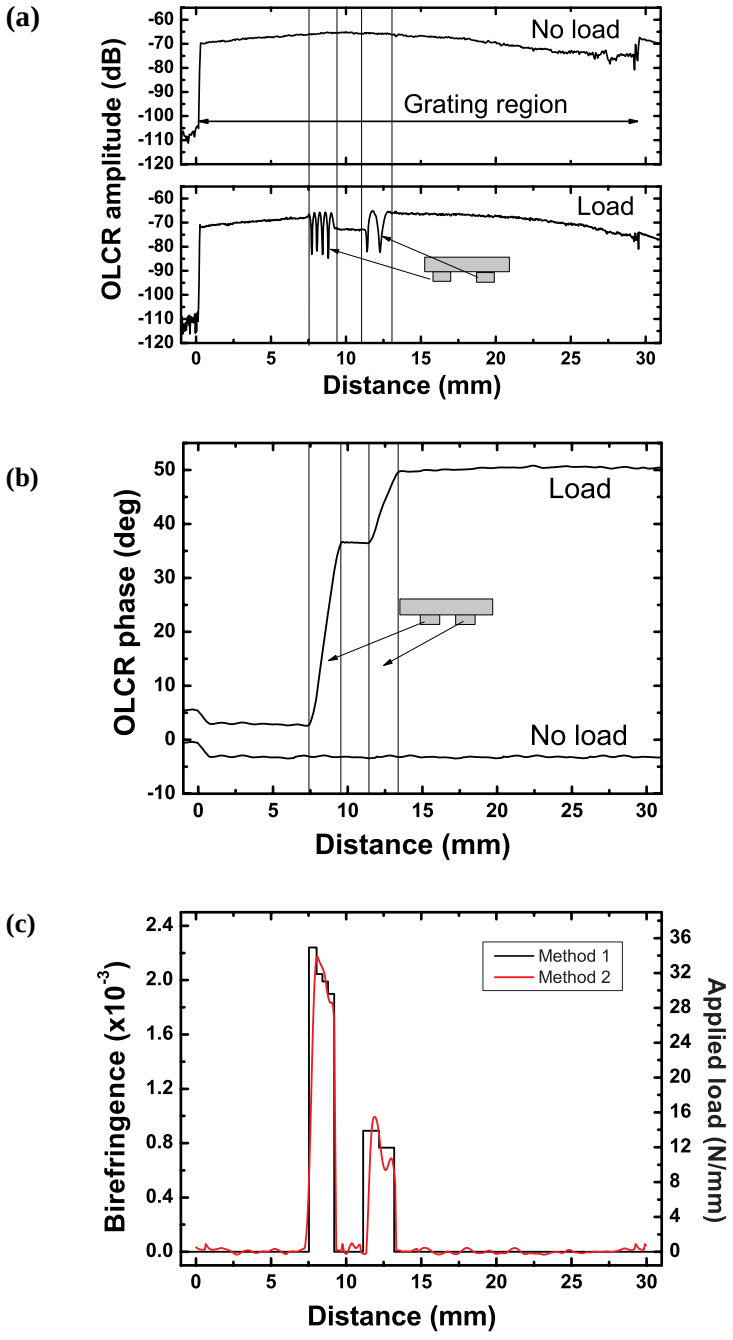


Fig. 5. Uniform FBG under local diametric loading (the loading element has two 2 mm sections separated by 2 mm) (a) OLCR amplitude (b) OLCR phase (c) Birefringence obtained from the amplitude (method 1) and the phase (method 2). The second y-axis is calculated using Eq. (7).

#74850 - $15.00 USD Received 7 September 2006; revised 7 November 2006; accepted 8 November 2006

## 4. Conclusions

In summary, we presented two novel methods for the measurement of local birefringence of FBGs using OLCR. The first technique uses oscillations in the OLCR amplitude signal to directly obtain the beat length and the birefringence. The spatial resolution is given by half the beat length in this case. This measurement could be performed with a simple non-phase sensitive setup, which offers significant advantages compared to methods such as OFDR that uses amplitude and phase measurement together with Fourier transformation to obtain similar information. The second method is based on the measurement of OLCR amplitude and phase together with inverse scattering to determine the effective Bragg wavelength along the grating. This method requires two independent measurements and mathematical reconstruction, but provides a very high spatial resolution limited by the coherence length of the light source and the data filtering function.

Both methods were compared with birefringence obtained from spectral measurements, and very good agreement was obtained. The application of both methods for the measurement of load induced local FBG birefringence was demonstrated showing advantages over classical spectral methods.

## Acknowledgments

The authors acknowledge the Swiss National Science Foundation (grant no. 068279) and the Swiss Federal Office for Education and Science (EU PLATON project no. 02.0271) for financial support.

#74850 - $15.00 USD Received 7 September 2006; revised 7 November 2006; accepted 8 November 2006